Impact of annealing cycle parameters on Batch Annealing process performance in tinplate manufacturing

Schoina L[*], Jones R[**], Burgess S[**], Vaughan D[**], Andrews L[**], Foley A[**], Valera-Medina A[*]
SchoinaL@cardiff.ac.uk
*College of Physical Sciences and Engineering, Cardiff University, UK
**Tata Steel UK Ltd, Trostre Works, Llanelli, Carmarthenshire, SA14 9SD, UK

Abstract

Research efforts in recent decades have led to significant improvements in steel manufacturing processes and energy efficiency; however, there still are opportunities for improvement, regarding product quality and material properties consistency and minimisation of material rejection. Therefore, the present study investigates the performance improvement of Batch Annealing furnaces used for steel substrate coil processing during tinplate manufacturing via heat transfer enhancement and alteration of annealing cycle parameters. At present, heat transfer to the coils is non-uniform, leading to non-uniform temperature profiles and recrystallisation across the coils, impacting the final tinplate product quality. This study first examined the current furnace by steady-state Computational Fluid Dynamics (CFD) analysis and validated the CFD model by comparison to existing industry thermocouple data for the steel coil in furnace position 2. Then, four proposed annealing furnace improvement scenarios were modelled in steady-state CFD analysis, with two cases each. The 5 and 10^{o}C soaking temperature increase cases showed a linear increase to the temperatures at the three coil areas. The two hydrogen percentage increase cases for the furnace atmosphere exhibited a smaller increase in the temperatures inside the coil, but the 14% hydrogen case showed an improved coil temperature uniformity. The four-times higher coiling tension results in an almost identical coil temperature profile to the 5^{o}C soaking temperature increase case, due to increased coil radial conductivity, and both four- and two-times higher coiling tensions showed the highest temperature uniformity. Finally, the 50% higher and lower silicate layer thickness cases showed almost no effect on the coil temperature profile and uniformity. Overall, the most promising furnace improvement scenarios are the higher coiling tension and higher soaking temperature cases, due to highest potential for better steel recrystallisation and final product quality, with the four-times higher coiling tension more promising for industrial implementation due to lower furnace running costs.

Introduction

Steel is one of the most important materials in modern societies as it is used in all aspects of everyday life, with its demand continuously increasing. One of the very common uses of steel is in tinplate manufacturing, where a thin, cold-reduced low-carbon steel sheet is coated on both sides with commercially pure tin [1]. The final product (Figure 1), the tinplate, is used mainly in packaging applications (cans) due to the combination of the strength and formability of steel with the corrosion resistance, paintability/printability and metallic lustre appearance of tin [2]. Tinplate manufacturing is divided into two stages: the steel strip production process to develop the required steel substrate characteristics, that consists of pickling, cold rolling, cleaning, annealing and tempering of hot rolled steel coils, and the electrolytic tin coating process [3].

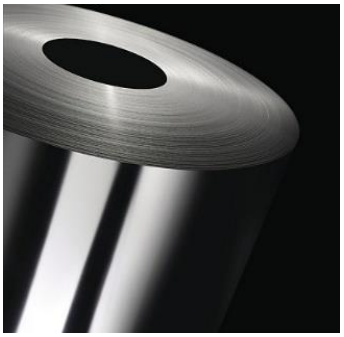

Figure 1. Final tinplate product [4].

After cold rolling, the steel becomes harder and stronger but more brittle; in order to restore the crystallography, relieve stresses and regain the necessary ductility, the steel is annealed either in a continuous line or in batch annealing furnaces, depending on the desired properties [3]. Batch annealing, which is of interest, is a non-continuous process, with four or five coils being annealed each time in batches for about three days. The coils are stacked with convector plates between them, covered by an inner cover containing protective atmosphere (93% nitrogen-7% hydrogen) and then are covered by an outer cover-furnace, where tangential natural gas burners are fired to provide the necessary heat for the process (Figure 2) [5]. The annealing cycle consists of three stages: heating, soaking at high temperature of above 600^{o}C and cooling. During heating, the point defects and dislocations, that previously created the large lattice distortions during cold rolling, are rearranged into a lower energy configuration and as a result the internal residual stresses are largely relieved [6]. As temperature increases further, recrystallisation begins with the nucleation and growth of new grains and the elimination of almost all remaining dislocations [7] and is considered complete when the steel mechanical properties become the same as before cold rolling, usually before the end of soaking [8].

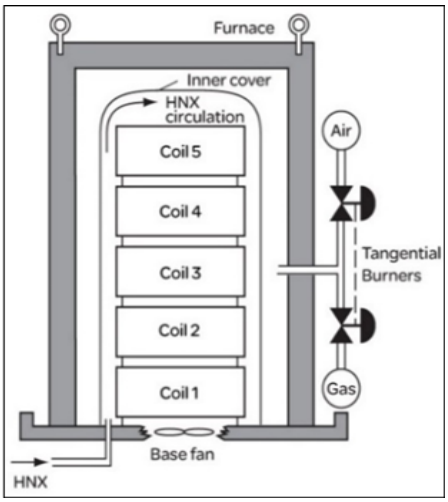

Figure 2. Batch annealing furnace with natural gas burners and nitrogen/hydrogen protective atmosphere [9].

For the batch annealing furnace and steel grade of interest in tinplate manufacturing, recrystallisation is considered successful when the temperatures inside the coils reach above 580^{o}C everywhere [10]. This temperature also ensures an interlap bonding (welding) between adjacent coil laps due to the temperature-driven diffusion of the sodium silicate layer previously deposited on the strip surfaces in the cleaning line, with this controlled breakdown resulting in an appropriate level of sticking between laps that will hold the coil together and impart some tension during uncoiling later at the start of the tempering line [10].

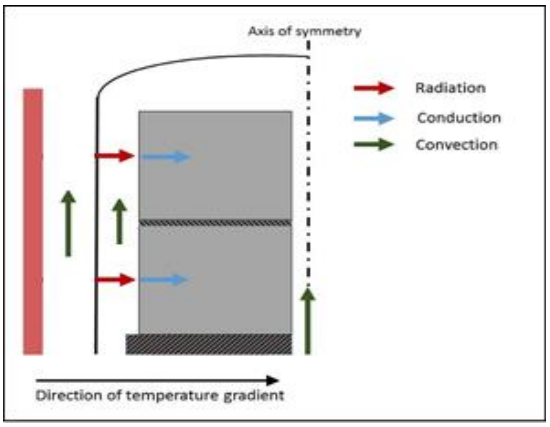

Figure 3. Heat transfer in batch annealing furnace during heating segments [11].

Inside the inner cover of the annealing furnace all three modes of heat transfer take place (Figure 3): radiation between the hot inner cover and the steel coils, conduction through the coil stack and forced convection between the moving protective atmosphere (by the base fan) and the cover and coil surfaces [12]. Batch annealing has, however, an inherent process inefficiency, the non-uniform heating of the steel coils, where the outer coil gets heated up more quickly and exposed to heat for

longer while waiting for cold spots inside the coil to reach the necessary recrystallisation temperature [13]. This happens due to the large mass of steel being annealed and the much slower conduction of heat in the coil's radial direction due to thermal resistance by silicate and air gap layers between adjacent steel coil laps [13]. The non-uniform coil temperature profile can lead to non-uniform material properties and surface defects, such as damage from the sticking of adjacent laps due to too much interlap welding or scratching caused by the relative movement of coil laps not held sufficiently together after annealing due to not enough interlap welding [14]. These can impact the final tinplate product quality and lead to significant amounts of material being disposed [10]. Improving the heat transfer processes in the furnace and altering annealing cycle operating parameters could potentially minimise non-uniformity in the coil temperature profiles therefore minimising defects and material and financial losses.

Increased soaking temperature could ensure steel recrystallisation completes successfully everywhere in the coil before the soaking segment ends due to higher temperatures achieved inside the coils and the temperature-dependent nature of the interlap bonding phenomenon [15]. However, temperature can increase by only so much, as too high temperatures can lead to over-annealing and different steel mechanical properties, especially on the outer coil that is more exposed to high heat [10]. Furthermore, increased soaking time by a few hours could also ensure the same result, as it could allow more time for heat to be conducted through the coil and the cold spots to 'catch up' with the higher temperatures in the outer coil; however, if too much time is added, over-annealing could again take place and it could also mean lower productivity for the batch annealing furnace [15].

Ensuring recrystallisation and more uniform temperature profiles could also be achieved by enhancing the convection heat transfer from the furnace atmosphere towards the coils. By increasing the hydrogen content of the protective atmosphere, its thermal conductivity increases since hydrogen's thermal conductivity is 7 times higher than that of nitrogen; as a result, it transfers heat more efficiently to the outer coil surfaces and inside the coil lap air gaps where it is also flowing [16]. Convection heat transfer could also be improved by using a higher base fan speed to increase fluid velocity and inlet flow turbulence, which in turn increases the overall convection coefficient [17].

Finally, an improvement to the conduction heat transfer inside the coil, by increasing the coil's overall thermal conductivity, could lead to the colder spots reaching the required temperatures faster and potentially sufficient interlap bonding. Literature suggests that an increased coiling tension in the cleaning line before batch annealing could bring the coil laps closer, enhancing recrystallisation and bonding reaction kinetics during annealing and increasing the contact points while reducing the air gap between adjacent laps, thus reducing thermal resistance in the radial conduction of heat [17]. However, since tensions are mostly relieved inside the coils during the annealing process, the actual effect of this strategy is uncertain but remans promising if the interlap bonding starts before tensions are relieved [14]. Furthermore, a reduction of the silicate layer thickness deposited in the cleaning line before annealing could also improve theoretically the radial coil thermal conductivity due to less thermal resistance, whereas a thicker layer could hinder the conduction of heat; however, in practice the uniformity of the silicate layer deposition might be even more important for a better, uniform interlap bonding process that results in the necessary level of coil cohesion [18].

In theory, all those strategies seem promising to combat the issues faced by the industry today; however, a combination of computer modelling and furnace trials in industry could be employed to test all those scenarios against the actual gains in consistency, product quality and productivity of tinplate manufacturing. This study will examine some of the above scenarios by computer modelling, with the results serving as a guide for future industrial trials, minimising productivity and financial losses related to such large scale testing.

Methodology

The current batch annealing furnace is examined first by steady-state Computational Fluid Dynamics (CFD) analysis in ANSYS Fluent in order to validate the furnace model by comparison to existing thermocouple data from trials in Trostre Works. Validating the CFD model would mean better accuracy for the analysis of furnace improvement scenarios later. More specifically, the comparison is based on the steel coil temperature profile of the coil in position 2, which is the second from the bottom of the stack, as most thermocouple data concern that coil position. A grid independence study is also conducted to verify that the CFD solution does not change depending on mesh size and structure. Next, four proposed furnace improvement scenarios are examined also in steady-state CFD analysis.

Computational Fluid Dynamics (CFD)

Computational Fluid Dynamics predicts fluid flow, heat transfer and other phenomena by solving numerically the governing equations of fluid dynamics: the mass, momentum and energy conservation equations presented below [19].

The mass conservation equation below states that the rate at which a mass enters a system equals the rate at which the mass is leaving the system plus the rate of accumulation of mass inside the system, where ρ is the density of the fluid (=mass/volume) and u, v, w are the three-dimensional fluid velocities [20]:

$$\frac{\partial \rho}{\partial t} + \frac{\partial \rho u}{\partial x} + \frac{\partial \rho v}{\partial y} + \frac{\partial \rho w}{\partial z} = 0$$

The momentum conservation (or Navier Stokes) equations below state that the rate of change of momentum of fluid particles in a controlled volume of fluid equals the sum of forces upon the fluid particles, where the ρ (Du,v,w)/ (Dt) components are the rates of change of momentum, the ρf terms represent the forces on the fluid (buoyancy and gravitational forces), p is the pressure applied on the compressible fluid flow and μ is the dynamic viscosity of the fluid [20], [21]:

x-component: $\rho \frac{Du}{Dt} = -\frac{\partial p}{\partial x} + \frac{\partial \tau_{xx}}{\partial x} + \frac{\partial \tau_{yx}}{\partial y} + \frac{\partial \tau_{zx}}{\partial z} + \rho f_x = -\nabla p + \mu \nabla^2 u + \rho f_x$

y-component: $\rho \frac{Dv}{Dt} = -\frac{\partial p}{\partial y} + \frac{\partial \tau_{xy}}{\partial x} + \frac{\partial \tau_{yy}}{\partial y} + \frac{\partial \tau_{zy}}{\partial z} + \rho f_y = -\nabla p + \mu \nabla^2 v + \rho f_y$

z-component: $\rho \frac{Dw}{Dt} = -\frac{\partial p}{\partial z} + \frac{\partial \tau_{xz}}{\partial x} + \frac{\partial \tau_{yz}}{\partial y} + \frac{\partial \tau_{zz}}{\partial z} + \rho f_z = -\nabla p + \mu \nabla^2 w + \rho f_z$

The energy conservation equation below states that the rate of change of energy of a fluid particle equals the sum of the net rate of heat addition into the fluid and of the net rate of work done on the fluid particle due to body and surface forces, where $\rho \frac{DE}{Dt}$ is the rate of change of energy, $k\nabla^2 T$ is net rate of heat conduction through the element boundaries in the three dimensions, S_h is any other sources of energy and the rest are the net work done on the fluid particle, with the $-\nabla.(\rho u)$ term representing the body forces and the second term representing the vector of surface stresses applied to the fluid in three dimensions [22]:

$$\rho \frac{DE}{Dt} = k\nabla^2 T + S_h - \nabla.(\rho u) + \left[\frac{\partial(u\,\tau_{xx})}{\partial x} + \frac{\partial(u\,\tau_{yx})}{\partial y} + \frac{\partial(u\,\tau_{zx})}{\partial z} + \frac{\partial(v\,\tau_{xy})}{\partial x} + \frac{\partial(v\,\tau_{yy})}{\partial y} + \frac{\partial(v\,\tau_{zy})}{\partial z} + \frac{\partial(w\,\tau_{xz})}{\partial x} + \frac{\partial(w\,\tau_{yz})}{\partial y} + \frac{\partial(w\,\tau_{zz})}{\partial z}\right]$$

A complex geometry is divided into a number of small control volumes (mesh) and, usually, the finite volume method is used to integrate the partial differential governing equations over the mesh's control volumes, with the variable of interest located at the centroid of each one (node), and thus creates discretised equations [23]. The unknown variables are approximated in order to transform the partial differential equations into linear algebraic equations, that are then solved iteratively to obtain the final solution for all nodal points [22]. The accuracy of the CFD solution depends on how close it is to the exact solution of the differential equations and commonly improves with higher mesh quality and amount of control volumes; however, too fine meshes can lead to very high computational effort [23]. To obtain a final solution, convergence must be achieved, meaning that at each iteration the approximate solution moves increasingly closer to the exact solution until they are considered 'close enough' according to specified convergence criteria, such as monitored target variable values (e.g. outlet temperature) and the number of residuals that are tolerances the governing equations must obey to in all mesh cells, measuring the imbalance of the CFD solution [11]. Finally, depending on the nature of the problem and on whether changes in fluid motion and temperature with time need to be monitored or a time-averaged solution is acceptable, a transient or steady-state solution is selected respectively [24].

Steady-state CFD analysis of current batch annealing furnace

The CFD analysis is performed using the ANSYS Fluent modelling software and the model geometry consists only of the space inside the inner cover, where the nitrogen-hydrogen protective atmosphere is flowing, and the four steel coil and three convector plate stack. Computer resources and time constraints as well as the focus on steel recrystallisation during soaking, led to only the soaking

segment of the annealing cycle being examined, where the soaking temperature is not varying with time. Therefore, the furnace model is examined with steady-state (time-averaged) CFD analysis that can serve as an indication of validity of the input parameters and, therefore, used to improve the setup of the model without consuming too much computational time [24]. A tetrahedral mesh is used for the fluid domain for better solution accuracy, with more refined mesh close to fluid boundaries, and a hexahedral mesh is used for the coils and the convector plates, which reduces the total number of elements of the model [11]. The realisable k-ε turbulence model is used for this case as it provides better accuracy for the prediction of turbulence than the standard k-ε while it still has reduced computational effort and the focus remains on heat transfer fluxes [24]. The simpler Surface-to-Surface radiation model is used as it is assumed that the protective atmosphere does not contribute to radiation exchange (zero optical thickness) [24].

The analysis models the worst performing furnace type and steel substrate which are the 93% nitrogen-7% hydrogen batch annealing furnace and the T57 3564 steel grade coil with dimensions of 1700mm diameter and 1017mm strip width and 0.180 gauge [10]. Due to limitations of computer resources and time, some assumptions and simplifications were made, such as simplified geometrical features, no heat loss to the environment from the furnace, fully turbulent fluid flow, exclusion of the base fan with its turbulence effect incorporated in the inlet flow parameters and the inlet flow temperature effect on the coil temperature profile caused by the base fan exclusion being ignored later in the results analysis. The heat provided by the natural gas burners in the outer cover is modelled by a constant temperature of the inner cover during the soaking segment. Finally, the coil, consisting of consecutive layers of steel, silicates and air gap, is modelled as a solid body, with average material properties and anisotropic thermal conductivity [25]. The axial conductivity is considered that of steel, since most of the heat would be conducted through the steel and not through the other layers [25], and the radial conductivity is calculated by thermal resistance circuit theory depending on the relative quantities of the layers (Figure 4) based on the equation below, where t and k are the corresponding layer thicknesses and thermal resistances respectively, $k_{r,eq}$ the total coil radial conductivity and A the percentage contact between coil laps [26], [27]:

$$\frac{t_{total}}{k_{r,eq}} = \frac{t_{steel}}{k_{steel}} + \frac{2t_{silicate}}{k_{silicate}} + \frac{t_{gap}}{k_{steel}A_{contact\%} + k_{gas}(1 - A_{contact\%})}$$

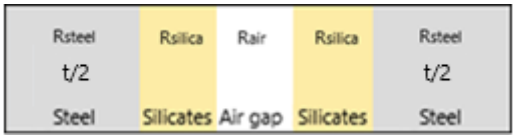

Figure 4. Layers of steel, silicates and air gap between adjacent coil laps [27].

The analysis is focused on the temperature profile of coil 2, the second from the bottom of the coil stack, as it is one of the coil positions with the worst product quality performance and therefore, there are more thermocouple data for it from industrial trials. Three positions in a coil cross-section at the middle of the coil's height are examined: the outer coil lap, the core lap and the cold spot area located at the one fourth of the radial distance from the coil core (Figure 5).

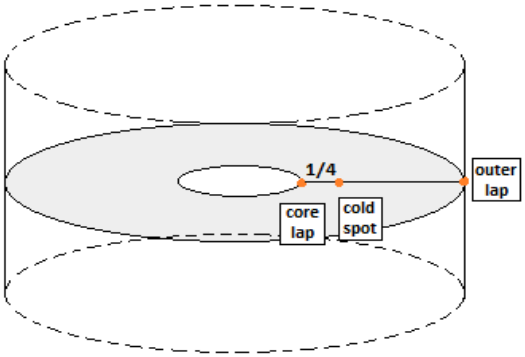

Figure 5. Core lap, cold spot and outer lap areas on a coil 2 cross-section at the middle of its height.

Grid independency study

Apart from convergence criteria used in the solving process, the solution must remain the same even if the mesh size/structure changes [11]. However, if the solution changes with the mesh then it is

not the correct solution even though the analysis appears to be converged and a new analysis has to be performed with finer mesh size, with the domain divided into more elements to improve accuracy [28]. For that purpose a grid independence study is performed by examining at least three mesh sizes while monitoring the value stability of an output variable of interest, with the solution considered acceptably converged when there is less than 1% difference from one to the next mesh size output variable solution [28].

Steady-state CFD analysis of furnace improvement scenarios

The validated steady-state CFD model is then used to examine four proposed furnace improvement scenarios, with two cases each: increased soaking temperature by 5ºC and 10ºC, increased hydrogen percentage in the furnace protective atmosphere from 7% to 10% and 14%, a two and four times increased coiling tension before batch annealing and a 50% higher and lower sodium silicate layer thickness deposited before annealing. The temperature profile of coil 2 is produced for each scenario and the results are compared to the current furnace case.

Results and Discussion

The results of the steady-state CFD analysis of the current batch annealing furnace and the four proposed furnace improvement scenarios are presented below. A comparison of the results takes place next, based on the highest coil temperatures achieved and on the highest temperature uniformity achieved inside coil 2.

Current furnace and CFD model validation

The results of the steady-state CFD analysis of the current batch annealing furnace are presented below, including the predicted temperature profile of coil 2 at the end of the soaking (Figure 6) and the comparison between the CFD results and thermocouple data (Table 1).

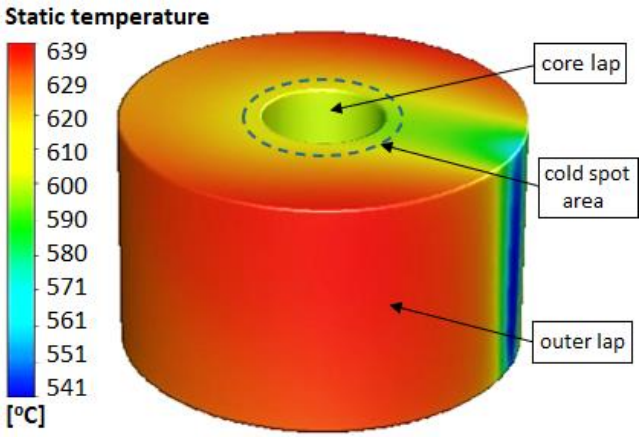

Figure 6. Coil 2 temperature profile of current furnace CFD results, showing core, cold spot and outer lap areas.

Table 1. Comparison of core, cold spot and outer lap temperatures between thermocouple data and CFD results.

Temperatures (ºC)	Thermocouple data	CFD model
Coil 2 – outer lap	642.3	639
Coil 2 – core lap	591.8	595
Coil 2 – cold spot	589	585-603 (av. 594ºC)

In Figure 6 the cold inlet gas effect on the coil temperature is visible, with colder temperatures at that side of the coil, but as a simplification to the model geometry it will not be considered in the results analysis. The maximum coil temperature at the outer coil laps is around 639ºC, whereas the temperature of the core laps is around 595ºC, and the temperature of the cold spot area is between 585 and 603ºC, with an average of 594ºC. Table 1 suggests that the above temperatures do not match exactly the thermocouple data for coil 2 at the end of soaking, as the data suggests that the outer coils laps should be about 642.3ºC, the core laps around 591.8ºC and the cold spot about 589ºC. A small deviation from the data, however, was expected in the steady-state CFD results as they derive from a time-averaged solution [24]. Therefore, since the solution shows a realistic approach to furnace data and the error is less than 1%, the CFD solution and the furnace model are deemed acceptable.

Grid independence study

A grid independence study was performed to establish the CFD solution independence of any mesh size or structure changes. Three different mesh sizes were examined, coarse, medium and fine mesh with 8.5, 12.4 and 19.3 million elements respectively, and the output variable monitored for solution independence was the furnace outlet temperature. The computational effort of each mesh size model is presented in core-hours, that are the product of number of processors used by the hours of simulation running time [29]. Table 2 below summarises the grid independence study results.

Table 2. Grid independence study results for coarse, medium and fine mesh, comparing number of mesh elements, outlet temperature and CPU core-hours.

Mesh size	Number of elements	Outlet temperature (ºC)	CPU (core-hours)
Coarse	8.5 million	548	552
Medium	12.4 million	567.75	1104
Fine	19.3 million	568.12	1536

All mesh size solutions are considered acceptable in terms of convergence, as there is less than 1% difference from one to the next mesh size outlet temperature value [], with the coarse mesh producing slightly lower outlet temperature than the other two. The medium and fine meshes reach almost the same result for the outlet temperature, suggesting strong convergence of the CFD solution [28]. Finally, the CPU core-hours utilised for the CFD analysis indicate that the coarser the mesh, the less computational effort is. The combination of accuracy and computational effort results suggests that the medium mesh is the optimal compromise between the two.

Furnace improvement scenario 1: Increased soaking temperature

The first improvement scenario examined is the increased soaking temperature in the batch annealing furnace. Higher soaking temperature could mean higher temperatures inside the coil at the end of the soaking segment and possibly better steel recrystallisation and interlap bonding [15]. Two cases were modelled: an increase of five and ten degrees Celsius to the soaking temperature. The results of the steady-state CFD analysis are presented in Table 3 below in comparison to the current furnace CFD results for the outer lap, core lap and cold spot area of the coil in position 2. The results show that by increasing the soaking temperature of the annealing cycle, an almost linear increase to the temperatures of the three areas of coil 2 is observed, with a 5ºC increase in soaking temperature, for instance, meaning a 5ºC higher outer and core lap temperatures. This temperature increase achieved at the colder areas of the coil could potentially ensure recrystallisation is completed successfully everywhere, leading to higher final product quality.

Table 3. Comparison of coil 2 temperatures between current furnace and increased soaking temperature cases.

Temperatures (ºC)	Current furnace	+5ºC soaking temperature	+10ºC soaking temperature
Coil 2 – outer lap	639	643	648
Coil 2 – core lap	595	600	605
Coil 2 – cold spot	585-603	595-605	600-610

Furnace improvement scenario 2: Increased hydrogen percentage furnace atmosphere

The second furnace improvement scenario model is an increase of the hydrogen percentage in the furnace protective atmosphere, currently consisting of 7% hydrogen and 93% nitrogen. Higher hydrogen content could possibly lead to enhanced convection heat transfer from the furnace atmosphere to the coils, as the thermal conductivity of hydrogen is much higher than that of nitrogen [16]. An enhanced heat transfer in the furnace could mean more uniform temperature profiles and steel recrystallisation for the coils [16]. Two cases were examined, with 10% hydrogen and 90% nitrogen, and with 14% hydrogen and 86% nitrogen.

Table 4. Comparison of coil 2 temperatures between current furnace and increased hydrogen percentage cases.

Temperatures (ºC)	Current furnace 7%H_2, 93%N_2	10% H_2, 90%N_2	14%H_2, 86%N_2
Coil 2 – outer lap	639	640	640
Coil 2 – core lap	595	595	596
Coil 2 – cold spot	585-603	589-600	593-600

The results, presented in Table 4 above, show a small increase in coil temperatures in the three areas of interest for both cases and a slightly more uniform temperature profile inside the coil as the temperature difference between the hotter outer lap and the coldest spot is getting smaller with increasing hydrogen percentage. For example, that temperature difference for the current furnace is 639-585=54 whereas it is 640-589=51 for the 10% hydrogen case.

Furnace improvement scenario 3: Increased coiling tension

The third improvement scenario concerns an increase in coiling tension at the cleaning line, before batch annealing. Theoretically, higher coiling tension means that the compressive force on the coil laps increases, and successive laps come closer together creating more contact points [17]. This results in enhanced conduction heat transfer in the coil radial direction due to more surface-to-surface conduction at the contact points and smaller air gaps between the laps, leading to lower thermal resistance [17]. Two cases were modelled with an increase in tension from 50MPa, that is the current case, to two (100MPa) and four times (200MPa) higher respectively. The steady-state CFD results presented below in Table 5 show for both cases an almost unchanged outer lap temperature to the current furnace (about 639^{o}C) and much higher temperatures for the core lap and the cold spot area. These higher temperatures and also the reduced temperature differences inside the coil confirm the theoretical positive effect of higher coiling tension on coil conductivity and could potentially also mean improved steel recrystallisation at those more problematic coil areas.

Table 5. Comparison of coil 2 temperatures between current furnace and increased coiling tension cases.

Temperatures (^{o}C)	Current furnace 50MPa	Tension x2 (100MPa)	Tension x4 (200MPa)
Coil 2 – outer lap	639	639.3	639..5
Coil 2 – core lap	595	597	599
Coil 2 – cold spot	585-603	594-601	595-604

Furnace improvement scenario 4: Altered silicate layer thickness

The final improvement scenario regards the alteration of the sodium silicate layer thickness that is deposited on the steel strip in the electrolytic cleaning line before annealing. Currently, the layer thickness is about 50Å or 0.005μm [10]. A lower thickness would mean reduced thermal resistance in the conduction of heat in the radial direction of the coil, resulting possibly in higher temperatures and improved temperature uniformity inside the coil, whereas a higher thickness would result to a higher thermal resistance, possibly hindering the radial conduction of heat inside the coil [18]. Two cases were examined: a 50% reduction and a 50% increase of the silicate layer thickness. Table 6 summarises the coil 2 CFD results for the three coil areas. The outer lap and core lap temperatures remain unchanged in both cases, whereas there is a very slight cold spot temperature increase and decrease for the lower and higher thickness cases respectively. This could be explained by the radial steel conductivity not being influenced significantly by the silicate layer thickness in the thermal resistance circuit calculations, as the thickness value is very small (10^{-9} magnitude).

Table 6. Comparison of coil 2 temperatures between current furnace and altered silicate layer thickness cases.

Temperatures (^{o}C)	Current furnace, thickness 50Å	Silicate layer thickness -50%	Silicate layer thickness +50%
Coil 2 – outer lap	639	639	639
Coil 2 – core lap	595	595	595
Coil 2 – cold spot	585-603	585.2-603	584.8-603

Discussion

To better understand the overall effect of the proposed furnace improvement scenarios on the annealing cycle performance, two comparisons are made between all the scenarios: one based on the highest core lap and average cold spot temperatures at the end of the soaking segment and the other on the highest temperature uniformity achieved inside the coil, expressed by the smallest maximum temperature difference [17].

Table 7 below presents the scenarios in order of decreasing core lap and average cold spot temperatures, including a maximum temperature difference value for each scenario.

Table 7. Comparison of inner coil temperatures and maximum temperature differences for each CFD model case.

Enhancement scenarios	Coil 2 –T core lap (°C)	Coil 2 –average T cold spot (°C)	ΔT= Tcoil2 max – Tcoil2 min (°C)
+10°C soaking T	605	600-610 → 605	648-600 = 48
+5°C soaking T	600	595-605 → 600	643-595 = 48
Coiling tension x4	599	595-604 → 599.5	639.5-595 = 44.5
Coiling tension x2	597	594-601 → 597.5	639.3-594 = 45.3
14%H2, 86%N2	596	593-600 → 596.5	640-593 = 47
10% H2, 90%N2	595	589-600 → 594.5	640-589 = 51
Silicate thickness -50%	595	585.2-603 → 594.1	639-585.2 = 53.8
Current furnace	***595***	***585-603 → 594***	***639-585 = 54***
Silicate thickness +50%	595	584.8-603 → 593.9	639-584.8 = 54.2

For the first comparison of temperatures at the problematic coil areas, the 10°C soaking temperature increase scenario achieves the highest core lap and average cold spot temperature of 605°C, which is about 10°C higher than the current furnace case and could potentially ensure complete steel recrystallisation by the end of soaking. This linear temperature increase can be explained by the lagging temperatures inside the coil being able to 'catch up' due to the long soaking period [17]. However, increasing the soaking temperature too much could cause the outer coil to over-anneal due to the disproportionally higher temperatures on the outside of the coil and also could lead to much higher running costs for the batch annealing furnace [17].

In the order of decreasing problematic area temperatures, next is the 5°C increase case followed by the increased coiling tension cases. It can be observed that the four times higher coiling tension scenario produces almost the same temperature results as the 5°C soaking temperature increase. This can be explained by the fact that the much higher steel radial conductivity resulting from the higher coiling tension actually enables a faster heat transfer inside the coil, whereas the higher soaking temperature only increases the temperature difference between the outside and inside, without speeding up the inner coil heat transfer [17]. Therefore, between the two the coiling tension increase could be more promising for the industry due to possibly lower furnace operational costs for the same result.

Furthermore, both cases of increased hydrogen percentage in the furnace atmosphere exhibit little effect on the inner coil temperature profile, which can be explained by the much larger percentage of nitrogen in the gas mixture in combination with the much lower thermal conductivity of nitrogen, that result in only a small increase of coil conductivity [16]. The 14% hydrogen scenario, which doubles the original hydrogen percentage, shows an increase of 1°C for the core lap and 2.5°C for the average cold spot temperature. However, such a large increase in hydrogen content for a small effect on the temperature profile could be unrealistic for the industry due to higher safety requirements and operational costs [10].

Finally, the silicate layer thickness alteration case results show almost no effect on the coil temperature profile, which is justified by the fact that the layer thickness is too small to have a significant effect on the radial coil conductivity.

The second comparison of the improvement scenarios is based on the highest temperature uniformity achieved by measuring the maximum temperature differences between the hottest and coldest coil spot (here between outer lap and coldest spot). A smaller temperature difference translates into a more uniform temperature profile and possibly more uniform steel recrystallisation and batch annealed steel properties and, thus, less defects and better final product quality [17]. The scenario exhibiting the smallest temperature difference, therefore higher temperature uniformity, is the four times higher coiling tension case with 44.5°C difference between the outer and inner coil, followed closely by the two times higher coiling tension case, which was expected due to the much higher coil radial conductivity as mentioned before.

Next, the 14% hydrogen case shows a difference of 47°C and is closely followed by the two soaking temperature increase scenarios. This indicates that a convection heat transfer enhancement due to higher hydrogen thermal conductivity could produce a positive effect on the annealing process performance regarding product quality similar to a 5-10°C increase in furnace soaking temperature, due to a more uniform way of heating the coil.

Finally, the silicate layer thickness cases show almost no impact on the temperature uniformity inside the coil, with the temperature difference values being almost equal to the current furnace case, due to the small effect of the very thin layer thickness on the overall coil conductivity. However, since the chemical reactions involved in the steel coil annealing process, such as the breaking down of the sodium silicate layer and the interlap bonding that provides cohesion, holding the coil together, are not included in the CFD analysis, the alteration of the silicate thickness could still play a role in batch annealing performance improvement, which could only be studied in detail by industry trials [18].

Overall, the steady-state CFD analysis results suggest that the most promising cases for batch annealing performance enhancement are the increased coiling tensions in the cleaning line before annealing to bring the coil laps closer together creating higher overall radial thermal conductivity and temperature uniformity, and the higher soaking temperatures in the furnace to achieve much higher temperatures inside the coil and higher temperature uniformity. Both options seem to have the potential for creating the conditions for better steel recrystallisation and possibly enhanced product quality with less defects, with the coiling tension deemed more promising for implementation due to possibly much lower annealing process running costs. However, it is worth noting that during annealing most of the tensions inside the coil are relieved; therefore, the actual effect of a higher coiling tension prior to annealing on batch annealing performance and temperature profiles is uncertain, but could be significant if the tension is relieved after the bonding takes place [14]. Literature suggests that the way to ensure a positive effect on batch annealing performance is increasing tension even further, even ten times higher [14]. Therefore, since CFD modelling is based on assumptions and simplifications and can only approach the real conditions, industrial trials in the actual batch annealing furnace would be the next step in the strategy to verify any positive impact of higher coiling tensions shown in the CFD results, with tensions of at least four times higher than the current case suggested for further examination. Finally, a techno-economic analysis would be necessary in order to factor the overall cost effectiveness of the proposed improvement scenarios into the decision-making process.

Summary

This study examined via steady-state Computational Fluid Dynamics (CFD) analysis the effect of steel coil batch annealing process parameters on the furnace performance regarding coil temperature profiles and steel recrystallisation. First, the CFD model results of the current batch annealing furnace were validated by a grid independency study and by comparison to existing industry thermocouple data, with the temperature profile of the coil in furnace position 2 at three areas of interest in the coil, the outer lap, core lap and cold spot, found to be less than 1% different to the thermocouple data. Then, four annealing furnace improvement scenarios were examined in steady-state CFD analysis, with two cases each:

- Both 5 and 10^{o}C soaking temperature increase cases showed an almost linear increase to the temperatures at the three areas of coil 2, which could ensure steel recrystallisation is completed successfully across the coil.
- The hydrogen percentage in the 7% hydrogen 93% nitrogen furnace atmosphere was increased to 10% and 14%, with both cases exhibiting only a small increase in the temperatures inside the coil (up to 2.5^{o}C). However, the 14% case showed a reduction in the maximum temperature difference inside the coil, meaning steel recrystallisation and properties would be more uniform ensuring better product quality.
- The four times higher coiling tension scenario results in very similar coil temperature profile to the 5^{o}C soaking temperature increase case, due to a large increase in coil radial conductivity. Both four and two times higher coiling tensions showed the smallest temperature differences (44-45^{o}C) inside the coil, with the enhanced temperature uniformity meaning possibly better product properties.
- The 50% higher and lower silicate layer thickness cases showed almost no effect on the coil temperature profile and on temperature uniformity due to the insignificant impact of the layer's small thickness on radial coil conductivity.

Overall, the most promising furnace improvement scenarios are the four times higher coiling tension and both higher soaking temperature cases, as they show the most potential for better steel recrystallisation conditions and enhanced final product quality, with the higher coiling tension deemed more promising for industrial implementation due to possibly much lower annealing process running costs.

References

[1] E. Morgan, “Tinplate Manufacture,” in *Tinplate & Modern Canmaking Technology*, 1st ed., Exeter: Pergamon Press, 1985, pp. 5-73,200-222.

[2] JFE Steel Corporation, “Tin Mill Products. [unknown],” Tokyo.

[3] ITRA Ltd, *Guide to Tinplate*, 2nd ed. Uxbridge: ITRA Ltd, 2000.

[4] Tata Steel, “Packaging Steel - Tinplate,” 2020. https://www.tatasteeleurope.com/en/products/packaging/tinplate (accessed Mar. 20, 2020).

[5] SMS group GmbH, “Efficient Production of Tinplate Packaging Material Out of Cold-Strip,” Hilden, 2015.

[6] ASM International, “Subject Guide: Heat Treating,” Ohio, 2015. [Online]. Available: www.asminternational.org.

[7] D. T. Llewellyn and R. C. Hudd, “Low-carbon strip steels,” in *Steels*, 3rd ed., D. T. Llewellyn and R. C. Hudd, Eds. Swansea: Butterworth-Heinemann, 1998, pp. 1–136.

[8] K. K. Alaneme and E. A. Okotete, “Recrystallization mechanisms and microstructure development in emerging metallic materials: A review,” *J. Sci. Adv. Mater. Devices*, vol. 4, no. 1, pp. 19–33, 2019, doi: 10.1016/j.jsamd.2018.12.007.

[9] Eurotherm Limited, “Single and multi-stack batch annealing,” England, 2006. Accessed: Mar. 20, 2020. [Online]. Available: https://www.eurotherm.com/download/ht-single-multi-stack-batch-annealing-app-note-hr084054u003/.

[10] Trostre Works Tata Steel Packagigng, “Personal communications.” Llanelli, 2020.

[11] Hadawi Fatla Oula M., “Development of Convection in High-Temperature Coil Annealing Furnaces Using Rotating Cylinders Technique [PhD Thesis],” Cardiff: Cardiff University, 2019.

[12] S. S. Sahay, R. Mehta, S. Raghavan, R. Roshan, and S. J. Dey, “Process analytics, modeling, and optimization of an industrial batch annealing operation,” *Mater. Manuf. Process.*, vol. 24, no. 12, pp. 1459–1466, 2009, doi: 10.1080/10426910903179922.

[13] J. A. Clifford, “The partial annealing of Low-Carbon Steel Strip [M.Sc. Thesis],” Montreal: McGill University, 1969.

[14] J. J. Bertrandie, L. Bordignon, P. D. Putz, and G. Volger, “Hot and cold rolling processes - Sticking and scratching problems after batch annealing, including coil compression stress effects,” Luxembourg, 2006.

[15] S. S. Sahay, B. V. H. Kumar, and S. J. Krishnan, “Microstructure evolution during batch annealing,” *J. Mater. Eng. Perform.*, vol. 12, no. 6, pp. 701–707, 2003, doi: 10.1361/105994903322692510.

[16] Y. Zuo *et al.*, “A study of heat transfer in high-performance hydrogen bell-type annealing furnaces,” *Heat Transf. - Asian Res.*, vol. 30, no. 8, pp. 615–623, 2001, doi: 10.1002/htj.10007.

[17] A. Buckley, A. J. Moses, and L. Trollope, “Study and redesign of high temperature batch annealing furnace for production of grain oriented electrical steel,” *Ironmak. Steelmak.*, vol. 26, no. 6, pp. 477–482, 1999, doi: 10.1179/030192399677338.

[18] L. Bordignon, P. Bastin, and M. Lamberigts, “Silica film deposition control during alkaline electrocleaning,” *Rev. Met. Paris*, vol. 93, no. 4, pp. 581–587, 1996, doi: https://doi.org/10.1051/metal/19969304058.

[19] P. J. Roache, *Computational Fluid Dynamics*, 1st ed. Albuquerque: Hermosa Publishers, 1972.

[20] J. D. Anderson, “Governing equations of fluid dynamics,” in *Computational Fluid Dynamics*, 1st ed., J. F. Wendt, Ed. Berlin: Springer-Verlag Berlin Heidelberg, 2009, pp. 15–51.

[21] P. R. N. Childs, *Rotating Flow*, 1st ed. Oxford: Elsevier, 2011.

[22] H. K. Versteeg and W. Malalasekera, *An Introduction to Computational Fluid Dynamics: The finite volume method*, 2nd ed. Harlow: Pearson Education Limited, 2007.

[23] J. H. Ferziger and M. Peric, *Computational Methods for Fluid Dynamics*, 3rd ed. [unknown]: Springer-Verlag Berlin Heidelberg, 2002.

[24] T. Hân, *ANSYS Fluent Theory Guide 15.0*. Canonsburg: ANSYS Inc, 2013.

[25] S. I. Barry and W. L. Sweatman, “Modelling heat transfer in steel coils,” *ANZIAM J.*, vol. 50, pp. 668–681, 2008, doi: 10.21914/anziamj.v50i0.1429.

[26] A. Saboonchi and S. Hassanpour, “Simulation of cold rolled steel coil heating during batch annealing process,” *Heat Transf. Eng.*, vol. 29, no. 10, pp. 893–901, 2008, doi: 10.1080/01457630802125807.

[27] M. Karlberg, *Thermo-Mechanical Modelling of Hot Strip Coil Cooling Process*, 1st ed. Lulea: Lulea University of Technology, 2014.

[28] Leap Australia, “Tips and tricks: Convergence and mesh independece study,” *Leading Engineering Application Providers*, 2021. https://www.computationalfluiddynamics.com.au/convergence-and-mesh-independent-study/ (accessed Nov. 08, 2021).

[29] Supercomputing Wales portal, “Guidance for completing the project application form on MySCW,” *Supercomputing Wales portal*, 2021. https://portal.supercomputing.wales/index.php/getting-access/guidance-for-completing-the-project-application-form-on-myscw/ (accessed Nov. 08, 2021).